

# Spin-glass behavior in $\text{Pr}_{0.7}\text{Ca}_{0.3}\text{CoO}_3$ and $\text{Nd}_{0.7}\text{Ca}_{0.3}\text{CoO}_3$

Asish K. Kundu<sup>a,b</sup>, P. Nordblad<sup>b</sup>, C.N.R. Rao<sup>a,\*</sup>

<sup>a</sup>Chemistry and Physics of Materials Unit, Jawaharlal Nehru Centre for Advanced Scientific Research, Jakkur P.O., Bangalore-560064, India

<sup>b</sup>Department of Engineering Sciences, Uppsala University, 751 21 Uppsala, Sweden

Received 4 October 2005; received in revised form 21 November 2005; accepted 11 December 2005

Available online 20 January 2006

## Abstract

With a view to investigate the effect of small size of *A*-site cations on the magnetic properties of the rare earth cobaltates,  $\text{Ln}_{1-x}\text{A}_x\text{CoO}_3$  (*Ln* = rare earth, *A* = alkaline earth), we have investigated  $\text{Pr}_{0.7}\text{Ca}_{0.3}\text{CoO}_3$  and  $\text{Nd}_{0.7}\text{Ca}_{0.3}\text{CoO}_3$  in detail. For this purpose, we have carried out low-field DC magnetization and ac susceptibility measurements including a study of magnetic relaxation and memory effects. Both  $\text{Pr}_{0.7}\text{Ca}_{0.3}\text{CoO}_3$  and  $\text{Nd}_{0.7}\text{Ca}_{0.3}\text{CoO}_3$  show frequency-dependent transitions at 70 and 55 K respectively in the ac susceptibility data, due to the onset of spin-glass like behavior. Their relaxation behavior exhibits aging effects. In addition, memory effects are found in the magnetization behavior. These characteristics establish spin-glass behavior in both these cobaltates, a behavior that is distinctly different from that of  $\text{La}_{0.7}\text{Ca}_{0.3}\text{CoO}_3$  and  $\text{La}_{0.5}\text{Sr}_{0.5}\text{CoO}_3$  which show well-defined ferromagnetic transitions, albeit without long-range ordering.

© 2005 Elsevier Inc. All rights reserved.

**Keywords:** Rare earth cobaltates; Magnetic properties; Spin-glasses

## 1. Introduction

Rare earth cobaltates of the type  $\text{Ln}_{1-x}\text{A}_x\text{CoO}_3$  (where *Ln* = rare earth, *A* = alkaline earth) show interesting magnetic and electron transport properties which are sensitive to the average radius of the *A*-site cations,  $\langle r_A \rangle$  [1–8]. Some of the compositions show characteristics of ferromagnets, but the ferromagnetism in these materials is generally not associated with long-range order. Magnetic properties of these cobaltates are instead considered to be akin to those of cluster or spin-glasses [4–6]. In this context, the recent study of cobaltates of the type  $\text{La}_{0.7-x}\text{Ln}_x\text{Ca}_{0.3}\text{CoO}_3$ , suggesting the coexistence of large ferromagnetic (FM) clusters along with smaller non-FM clusters is noteworthy [5]. While  $\text{La}_{0.7}\text{Ca}_{0.3}\text{CoO}_3$  shows a behavior somewhat like a FM material with a marked increase in magnetization around 170 K,  $\text{Pr}_{0.7}\text{Ca}_{0.3}\text{CoO}_3$  and  $\text{Nd}_{0.7}\text{Ca}_{0.3}\text{CoO}_3$  with smaller  $\langle r_A \rangle$  values, do not show such distinct FM transitions [5,7,8]. The last two cobaltates exhibit low magnetization values down to low temperatures and an inhomogeneous magnetic behavior [8]. In

order to understand the nature of magnetism in these cobaltates, we have carried out a detailed study on single crystals at low fields along different directions, in addition to ac susceptibility and relaxation measurements. The study establishes that both  $\text{Pr}_{0.7}\text{Ca}_{0.3}\text{CoO}_3$  and  $\text{Nd}_{0.7}\text{Ca}_{0.3}\text{CoO}_3$  behave dynamically as spin-glasses at low temperatures.

## 2. Experimental procedure

Single crystals of  $\text{Pr}_{0.7}\text{Ca}_{0.3}\text{CoO}_3$  and  $\text{Nd}_{0.7}\text{Ca}_{0.3}\text{CoO}_3$  were grown by the floating-zone furnace fitted with two ellipsoid halogen lamps, having prepared the polycrystalline rods (feed and seed) by conventional the solid-state reaction method, starting with stoichiometric mixtures of the rare earth oxides, with  $\text{CaCO}_3$  and  $\text{Co}_3\text{O}_4$ . The monophasic polycrystalline powders were hydrostatically pressed and sintered at 1473 K for 24 h in air to obtain feed and seed rods with a diameter of 3–4 mm and a length of 90–100 mm. Single crystals were grown under an oxygen flow of 2–4 l/min at a growth rate of 3–7 mm/h. Small parts of the crystals were cut off and ground to fine powder to record the X-ray diffraction pattern, using a Seifert 3000

\*Corresponding author. Fax: +91 2208 2760.

E-mail address: [cnrao@jncasr.ac.in](mailto:cnrao@jncasr.ac.in) (C.N.R. Rao).

TT diffractometer employing  $\text{CuK}\alpha$  radiation. The diffraction patterns show the cobaltates to have an orthorhombic structure ( $Pnma$  space group) with the unit cell parameters in agreement with the literature values [8]. Composition analysis carried out by using energy dispersive X-ray (EDX) analysis in LEICA S440I scanning electron microscope fitted with a Si–Li detector, gave the expected metal ratios. The oxygen stoichiometry was established to be close to three by iodometric titrations, within an error of  $\pm 0.02$ .

A Quantum Design MPMSXL SQUID magnetometer and a non-commercial low field SQUID magnetometer system [9] were used to investigate the magnetic properties of the single crystal. The temperature dependence of the zero-field-cooled (ZFC), field-cooled (FC) and thermoremanent magnetization (TRM) were measured in different applied magnetic fields. Hysteresis measurements were carried out at different temperatures. The dynamics of the magnetic response was studied by ac-susceptibility measurements at different frequencies and measurements of the relaxation of the low field ZFC magnetization.

While measuring the temperature dependence of the ZFC magnetization, the sample was cooled from 320 to 5 K in zero-field, the field applied at 5 K and the magnetization recorded on re-heating the sample. In the FC and TRM measurements, the sample was cooled in the applied field to 5 K and the magnetization recorded on re-heating the sample, keeping the field (FC procedure) or after cutting off the field (TRM procedure). In the relaxation experiments, the sample was cooled in zero-field from a reference temperature of 90 K (for Pr) and 70 K (for Nd) to a measuring temperature,  $T_m$  and kept there during a wait time,  $t_w$ . After the wait time, a small probing field was applied and the magnetization was recorded as a function of time elapsed after the field application.

### 3. Results and discussion

Fig. 1 shows the temperature dependence of the ZFC and FC magnetization of  $\text{Ln}_{0.7}\text{Ca}_{0.3}\text{CoO}_3$  ( $\text{Ln} = \text{La}$ , Pr and Nd) crystals measured parallel and perpendicular to the  $c$ -axis in an applied field of 20 Oe. The magnitudes of both  $M_{\text{FC}}(T)$  and  $M_{\text{ZFC}}(T)$  are higher in the perpendicular direction, the behavior remaining similar down to low temperatures.  $\text{La}_{0.7}\text{Ca}_{0.3}\text{CoO}_3$  shows a distinct FM type transition in the FC data around 170 K ( $T_C$ ) as expected, while the ZFC data show a cluster-glass transition around 95 K [10].  $\text{Pr}_{0.7}\text{Ca}_{0.3}\text{CoO}_3$  and  $\text{Nd}_{0.7}\text{Ca}_{0.3}\text{CoO}_3$  do not, however, show such a ferromagnet type behavior down to low temperatures. On the other hand, they only show a slight increase in magnetization with decreasing temperature around 70 K, but the magnetization reaches values much lower than the theoretical saturation values even at 5 K. The irreversible temperature,  $T_{\text{irr}}$ , between the ZFC and FC data in  $\text{Pr}_{0.7}\text{Ca}_{0.3}\text{CoO}_3$  and  $\text{Nd}_{0.7}\text{Ca}_{0.3}\text{CoO}_3$  persists up to 200 K unlike in the La derivative where they merge around  $T_C$ . The  $T_{\text{irr}}$ , however, decreases with the

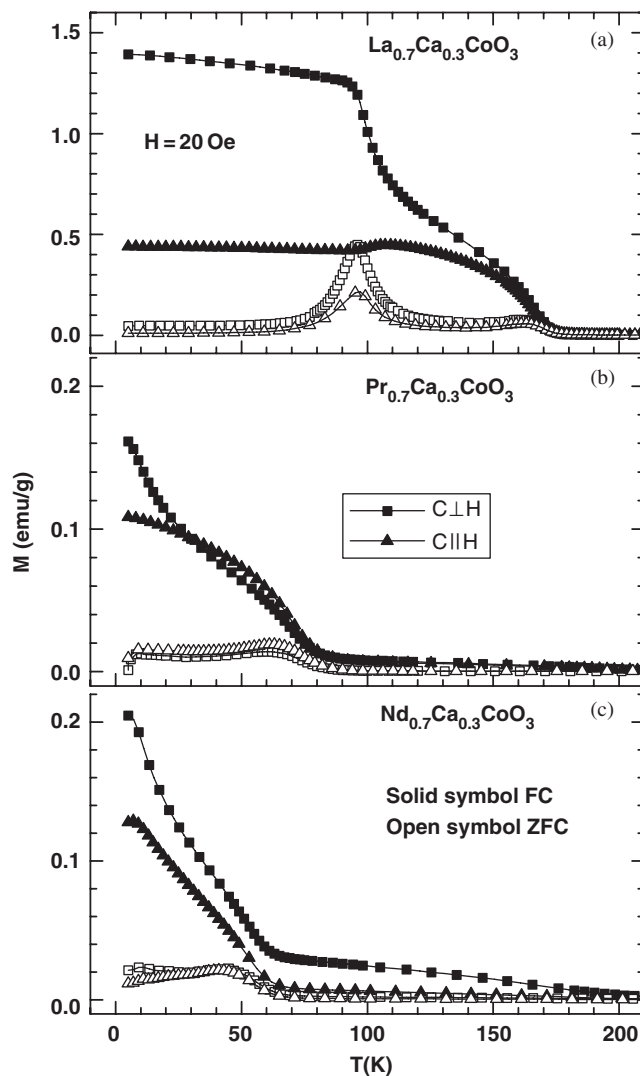


Fig. 1. Temperature dependence of the ZFC (open symbols) and FC (solid symbols) magnetization,  $M$ , of  $\text{Ln}_{0.7}\text{Ca}_{0.3}\text{CoO}_3$  where (a)  $\text{Ln} = \text{La}$  (b)  $\text{Ln} = \text{Pr}$  and (c)  $\text{Ln} = \text{Nd}$ , at  $H = 20$  Oe measured parallel (triangle symbol) and perpendicular (square symbol) to the  $c$ -axis.

increasing magnetic field. The TRM changes with temperature in a manner similar to the difference between the FC and ZFC magnetization.

Inverse magnetic susceptibility data of the cobaltates provide supporting information. The data could be fitted to Curie–Weiss behavior with the extrapolated Weiss temperatures,  $\theta_p$ , of 150,  $-180$  and  $-340$  K for the La, Pr and Nd-derivatives, respectively. The negative  $\theta_p$  values in the latter two cobaltates imply the presence of antiferromagnetic interactions in the high temperature region, while for La-derivative the interaction is FM.

Fig. 2 shows  $M$ – $H$  data of  $\text{Pr}_{0.7}\text{Ca}_{0.3}\text{CoO}_3$  and  $\text{Nd}_{0.7}\text{Ca}_{0.3}\text{CoO}_3$  at different temperatures, measured parallel to the  $c$ -axis of the samples. These cobaltates show hysteresis loops at low temperatures ( $\leq 10$  K) and a non-saturating behavior up to 5 Tesla (T). The values of the remanence magnetization and coercive field for the Pr

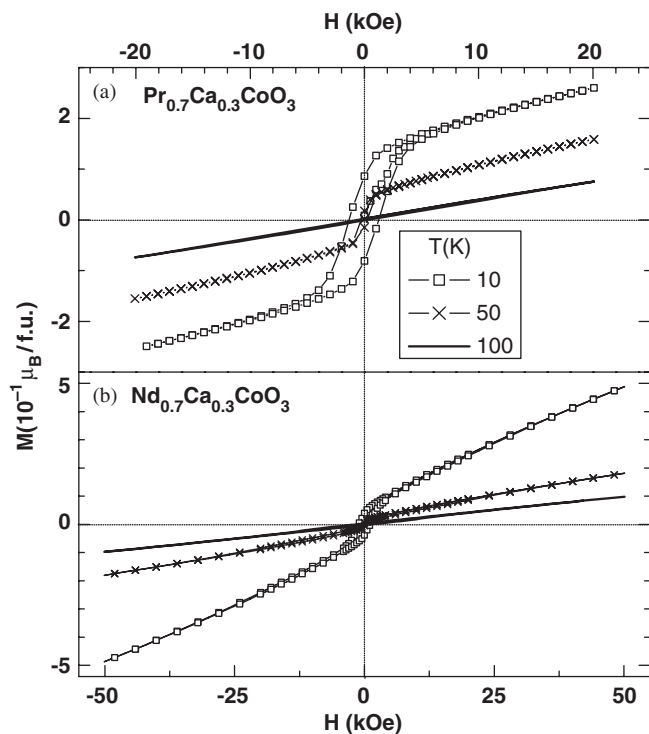


Fig. 2. The hysteresis curves for (a)  $\text{Pr}_{0.7}\text{Ca}_{0.3}\text{CoO}_3$  and (b)  $\text{Nd}_{0.7}\text{Ca}_{0.3}\text{CoO}_3$  at different temperatures measured parallel to the  $c$ -axis.

compound at 10 K are  $0.03 \mu_{\text{B}}/\text{f.u.}$  and 0.15 T, respectively, while those for the Nd derivative are  $0.01 \mu_{\text{B}}/\text{f.u.}$  and 0.12 T. The remanence magnetization and coercive field for  $\text{La}_{0.7}\text{Ca}_{0.3}\text{CoO}_3$  at 10 K are  $0.1 \mu_{\text{B}}/\text{f.u.}$  and 0.6 T, respectively [10]. In spite of the  $c$ -axis dependence of the low-field behavior, the high-field parts of the  $M$ – $H$  curves are nearly independent of the field direction. The coercive field and remanent magnetization are almost the same in both the orientations. With increasing temperature, the width of the hysteresis loop decreases rapidly and finally the  $M$ – $H$  behavior becomes linear at higher temperatures (see the 100 K curves in Fig. 2).

In order to further characterize the magnetic behavior of  $\text{Pr}_{0.7}\text{Ca}_{0.3}\text{CoO}_3$  and  $\text{Nd}_{0.7}\text{Ca}_{0.3}\text{CoO}_3$ , we have carried out ac susceptibility and magnetic relaxation measurements which are useful to investigate the magnetic glassy behavior [11,12]. Fig. 3 shows the temperature dependence of the in-phase ZFC magnetization,  $\chi'(T)$  and the out-of-phase  $\chi''(T)$  components of the ac-susceptibility for  $\text{Pr}_{0.7}\text{Ca}_{0.3}\text{CoO}_3$  and  $\text{Nd}_{0.7}\text{Ca}_{0.3}\text{CoO}_3$ . Both the systems show frequency-dependence below 80 K, down to low temperatures. A frequency-dependent maximum is observed around 70 K for  $\text{Pr}_{0.7}\text{Ca}_{0.3}\text{CoO}_3$  in the in-phase as well as the out-of-phase components as can be seen in Figs. 3(a) and (b). With increasing frequency, the peak value shifts toward higher temperatures.  $\text{Nd}_{0.7}\text{Ca}_{0.3}\text{CoO}_3$  shows a peak around 55 K as shown in Figs. 3(c) and (d). Thus, with decrease in the average radius of the  $A$ -site cations,  $\langle r_A \rangle$ , the magnetic transition temperature as revealed by the ac

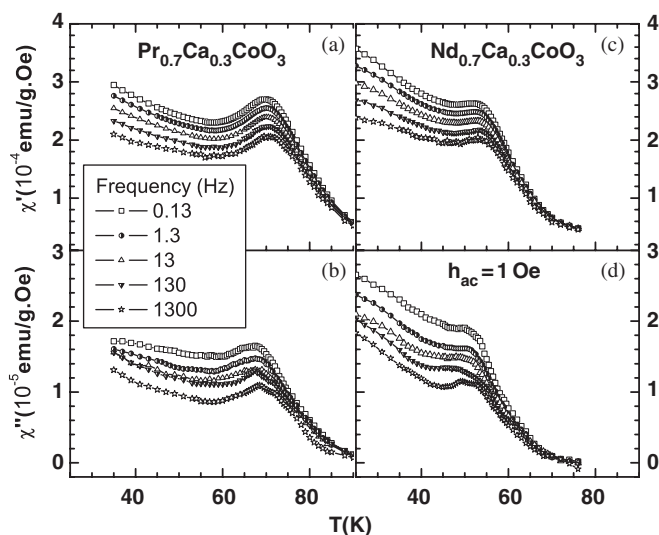


Fig. 3. The temperature dependence of the in-phase and out-of-phase ac-susceptibility for (a,b)  $\text{Pr}_{0.7}\text{Ca}_{0.3}\text{CoO}_3$  and (c,d)  $\text{Nd}_{0.7}\text{Ca}_{0.3}\text{CoO}_3$  at different frequencies ( $c$ -axis  $\parallel h_{\text{ac}}$ ).

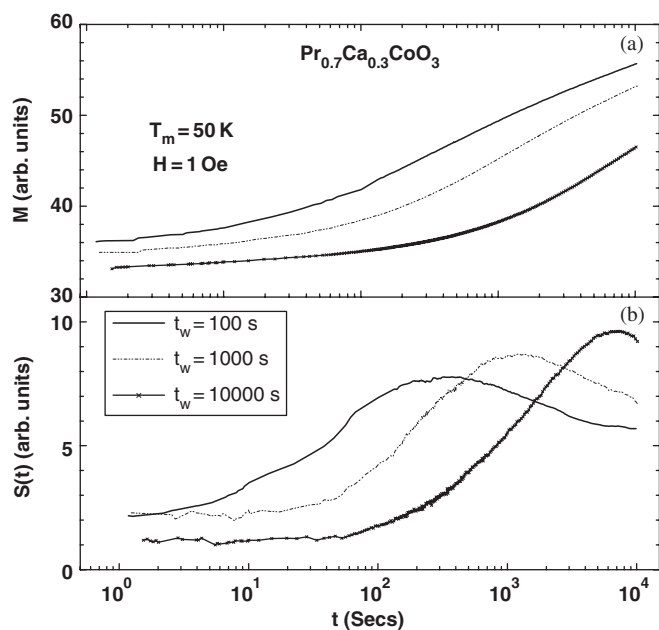


Fig. 4. ZFC-relaxation measurements on  $\text{Pr}_{0.7}\text{Ca}_{0.3}\text{CoO}_3$  at  $T_m = 50$  K for different waiting times,  $t_w = 100, 1000$  and  $10000$  s ( $c$ -axis parallel to the field,  $H = 1$  Oe).

susceptibility maximum shifts to lower temperatures. The ac susceptibility of the cobaltates found here is quite different from the non-linear behavior found in certain canted systems [13].

From the time-dependent ZFC magnetization measurements, we find that both  $\text{Pr}_{0.7}\text{Ca}_{0.3}\text{CoO}_3$  and  $\text{Nd}_{0.7}\text{Ca}_{0.3}\text{CoO}_3$  exhibit logarithmical dynamics below the transition temperature (70 and 55 K). Figs. 4(a) and (b) present the time-dependent relaxation of the ZFC magnetization for  $\text{Pr}_{0.7}\text{Ca}_{0.3}\text{CoO}_3$ , measured at 50 K ( $T_m$ ) and the

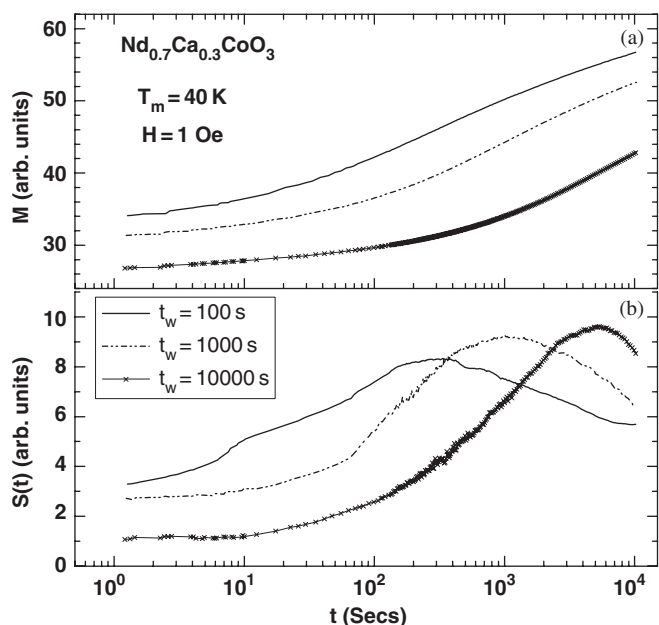


Fig. 5. ZFC-relaxation measurements on  $\text{Nd}_{0.7}\text{Ca}_{0.3}\text{CoO}_3$  at  $T_m = 40$  K for different waiting times,  $t_w = 100, 1000$  and  $10000$  s ( $c$ -axis parallel to the field,  $H = 1$  Oe).

corresponding relaxation rates  $S(t) = 1/H [dM_{\text{ZFC}}(T, t_w, t)/d\log_{10}(t)]$ . In all the ZFC-relaxation measurements, the applied field was 1 Oe and the wait times were  $t_w = 100, 1000$  and  $10000$  s. Results of similar measurements on  $\text{Nd}_{0.7}\text{Ca}_{0.3}\text{CoO}_3$  at 40 K are presented in Figs. 5(a) and (b). The relaxation rate attains a maximum at the elapsed time, close to the wait time, indicating a pronounced age-dependent effect. Such a behavior is generally observed in spin-glasses [11]. Such an effect is explained within the droplet (or domain growth) model, by associating the maximum in the relaxation rate with a crossover between quasi-equilibrium and non-equilibrium dynamics [14].

We have investigated memory effects using the ZFC magnetization vs. temperature experiments [15]. First, a reference experiment was made according to the ZFC protocol described earlier. Then, a memory curve was recorded, with the additional feature that cooling was halted at a stop temperature for some hours during which the sample ages (c.f. aging experiments). This slows down the dynamics at temperatures around the stop temperature, which sustains when the temperature is decreased, and appears as a dip in the  $M_{\text{ZFC}}(T)$  curve at the stop temperature on re-heating the sample. To clearly illustrate memory, it is convenient to plot the difference between the reference and the memory curve. It may be noted that a specific characteristic of a spin glass phase (ordinary or re-entrant) is the memory behavior, whereas a disordered and frustrated FM phase shows little or no memory effect. In the case of  $\text{Pr}_{0.7}\text{Ca}_{0.3}\text{CoO}_3$ , the experiments were carried (a) with a halt at 30 K, (b) with a halt at 50 K and (c) with halts at both 30 and 50 K. The weak DC field applied in the measurement does not affect the non-equilibrium process

intrinsic to the sample, but only works as a non-perturbing probe of the system. A memory effect is clearly observed as shown in Fig. 6(a) at 30 K, (b) at 50 K and (c) at both 30 and 50 K after direct cooling from 100 K. The memory dip appears even more prominently on subtracting the reference curve as shown in the inset of Fig. 6. The memory experiments on  $\text{Nd}_{0.7}\text{Ca}_{0.3}\text{CoO}_3$  at three different temperatures show similar results (see Fig. 7). In Fig. 7(a), we show

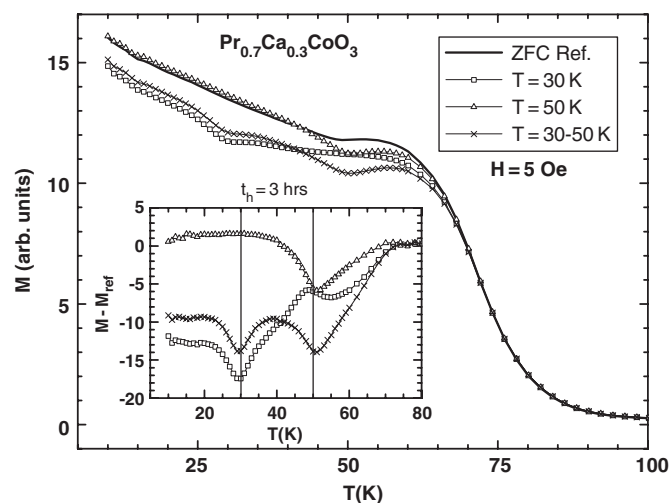


Fig. 6. The temperature dependence of ZFC magnetization,  $M$ , (reference curve) and on imprinting memories of  $\text{Pr}_{0.7}\text{Ca}_{0.3}\text{CoO}_3$  at two temperature stops (30 and 50 K) during cooling each for 3 h. The inset shows the difference ( $M - M_{\text{ref}}$ ) plot of the respective curves ( $c$ -axis parallel to the field,  $H = 5$  Oe).

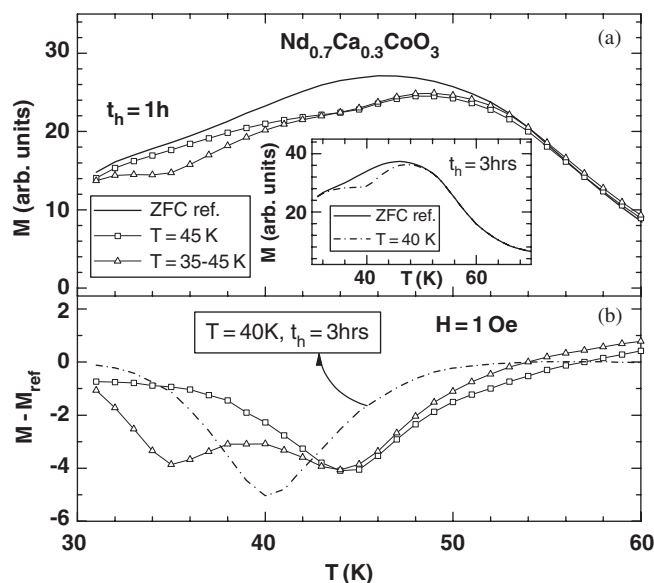


Fig. 7. ZFC magnetization memory experiment on  $\text{Nd}_{0.7}\text{Ca}_{0.3}\text{CoO}_3$ : (a) the temperature dependence of ZFC magnetization,  $M$ , (reference curve) and on imprinting memories of two temperature stops (at 35 and 45 K) during cooling each for 1 h and (b) the difference ( $M - M_{\text{ref}}$ ) plot of the respective curves ( $c$ -axis parallel to the field,  $H = 1$  Oe). The inset shows the memory curve corresponding to halting time 3 h ( $T = 40$  K).

the reference curve along with two memory curves with halts at 35 and 45 K, the inset corresponding to a halt at 40 K. We observe memory dips at the stop temperatures. The observed memory effects clearly establish that both  $\text{Pr}_{0.7}\text{Ca}_{0.3}\text{CoO}_3$  and  $\text{Nd}_{0.7}\text{Ca}_{0.3}\text{CoO}_3$  behave like spin-glasses at the low temperatures.

#### 4. Conclusions

Although cobaltates of the type  $\text{La}_{1-x}\text{Sr}_x\text{CoO}_3$  ( $x \geq 0.3$ ) were considered to be itinerant ferromagnets, recent studies have revealed that these cobaltates show magnetic phase separation wherein relatively large FM clusters or domains associated with a distinct  $T_C$ , coexist with small magnetic clusters showing glassy behavior [6].  $\text{La}_{1-x}\text{Sr}_x\text{CoO}_3$  compositions also show an insulator–metal transition with increasing  $x$  since the large FM clusters are metallic. A recent study of  $\text{La}_{0.7-x}\text{Ln}_x\text{Ca}_{0.3}\text{CoO}_3$  ( $\text{Ln} = \text{Pr}, \text{Nd}, \text{Gd}$  or  $\text{Dy}$ ) reinforces the phase separation scenario wherein large carrier-rich FM clusters and carrier-poor smaller clusters coexist [5,10]. Such magnetic phase separation would be expected to be sensitive to the size of  $A$ -site cations. As the size of the  $A$ -site cations decreases as in  $\text{Pr}_{0.7}\text{Ca}_{0.3}\text{CoO}_3$  and  $\text{Nd}_{0.7}\text{Ca}_{0.3}\text{CoO}_3$ , we would expect a situation where a small magnetic clusters to dominate, favoring glassy behavior. The present measurements show that both  $\text{Pr}_{0.7}\text{Ca}_{0.3}\text{CoO}_3$  and  $\text{Nd}_{0.7}\text{Ca}_{0.3}\text{CoO}_3$ , do not show any evidence of a ferromagnet-like magnetic behavior with well defined  $T_C$  associated with large FM clusters or domains, but instead behave like spin-glass at low temperatures. In other words, because of the small  $A$ -site cations radius,  $\langle r_A \rangle$ , these two cobaltates no longer represent phase-separated systems but are genuine spin-glasses. Accordingly, both these cobaltates are insulators. The behavior of the Pr and Nd cobaltates found here is quite different from that of  $\text{LaCo}_{1-x}\text{Ni}_x\text{O}_3$  which also exhibits FM interactions [16,17]. The properties of  $\text{Pr}_{0.7}\text{Ca}_{0.3}\text{CoO}_3$  found here are comparable to those reported by Tsubouchi et al. [18], but the interpretation of the results provided here in the light of the non-equilibrium properties is different.

#### Acknowledgments

Financial support for this work from the Swedish agencies SIDA/SAREC and VR through the Asian–Swedish research links Programme is acknowledged. The authors thank BRNS (DAE), India for support of this research. AKK thanks the University Grants Commission of India for a fellowship and Victor and Michael for their help with the SQUID measurements.

#### References

- [1] C.N.R. Rao, O. Parkash, D. Bahadur, P. Ganguly, S. Nagabhushana, *J. Solid State Chem.* 22 (1977) 353.
- [2] M.A.S. Rodriguez, J.B. Goodenough, *J. Solid State Chem.* 118 (1995) 323.
- [3] J.C. Burley, J.F. Mitchell, S. Short, *Phys. Rev. B* 69 (2004) 054401.
- [4] M. Itoh, I. Natori, S. Kubota, K. Matoya, *J. Phys. Soc. Japan* 63 (1994) 1486.
- [5] A.K. Kundu, K. Ramesha, R. Seshadri, C.N.R. Rao, *J. Phys.: Condens. Matter* 16 (2004) 7955.
- [6] J. Wu, C. Leighton, *Phys. Rev. B* 67 (2003) 174408; J. Wu, J.W. Lynn, C.J. Glinka, J. Burley, H. Zheng, J.F. Mitchell, C. Leighton, *Phys. Rev. Lett.* 94 (2005) 037201.
- [7] H. Masuda, T. Fujita, T. Miyashita, M. Soda, Y. Yasui, Y. Kobayashi, M. Sato, *J. Phys. Soc. Japan* 72 (2003) 873.
- [8] A.K. Kundu, E.V. Sampathkumaran, K.V. Gopalakrishnan, C.N.R. Rao, *J. Mag. Mag. Mater.* 281 (2004) 261.
- [9] J. Magnusson, C. Djurberg, P. Granberg, P. Nordblad, *Rev. Sci. Instr.* 68 (1997) 3761.
- [10] A.K. Kundu, P. Nordblad, C.N.R. Rao, *Phys. Rev. B* 72 (2005) 144423.
- [11] J.A. Mydosh, in: *Spin Glasses: An Experimental Introduction*, Taylor and Francis, London, 1993; K. Binder, A.P. Young, *Rev. Mod. Phys.* 58 (1986) 801.
- [12] L. Lundgren, P. Svedlinth, P. Nordblad, O. Beckman, *Phys. Rev. Lett.* 51 (1983) 911.
- [13] S. Mukherjee, R. Ranganathan, S.B. Roy, *Phys. Rev. B* 50 (1994) 1084.
- [14] D.S. Fisher, D.A. Huse, *Phys. Rev. B* 38 (1988) 373.
- [15] R. Mathieu, P. Jonsson, D.N.H. Nam, P. Nordblad, *Phys. Rev. B* 63 (2001) 092401.
- [16] J. Androulakis, N. Katsarakis, J. Giapintzakis, *J. Appl. Phys.* 91 (2002) 9952.
- [17] D. Hammer, J. Wu, C. Leighton, *Phys. Rev. B* 69 (2004) 134407.
- [18] S. Tsubouchi, T. Kyomen, M. Itoh, M. Oguni, *Phys. Rev. B* 69 (2004) 144406.